Bayram, I. S., & Galloway, S. (2022). Pricing-based distributed control of fast EV charging stations operating under cold weather. IEEE Transactions on Transportation Electrification, 8(2), 2618 - 2628. https://doi.org/10.1109/TTE.2021.3135788

Pricing-based Distributed Control of Fast EV Charging Stations Operating Under Cold Weather

I. Safak Bayram and Stuart Galloway

Abstract

As the electric vehicle (EV) adoption rates increase there is a pressing need for designing charging stations that accounts for heterogeneity (e.g. charging rates, duration) in EV demand. Battery temperature is a major factor determining the maximum charging rates as the EV charging power is limited to ensure the safety of batteries. As a consequence, each vehicle receives a different charging rate and the station can be modelled as a multi-class queuing facility. As the coverage of such networks grows the power network elements become more congested and controlling the charging demand is needed to avoid overloading. This paper models a network of fast chargers as a multi-dimensional loss system and proposes an EV load control framework that leverages pricing dynamics to keep the aggregate demand below station capacity with minimal loss of load (outage) events. The global problem is formulated to maximise the social welfare of all users, and optimal arrival rates are calculated in a distributed manner. The mathematical analysis further shows how to induce a socially optimal charging behaviour through the computation of congestion prices. The results show that class-specific prices provide fairness to EVs with colder batteries, as they receive slower service.

Index Terms

Electric Vehicles, Fast Charging, Cold Weather, Pricing based control.

I. Safak Bayram and Stuart Galloway are with the Department of Electric and Electrical Engineering, University of Strathclyde, Glasgow, G1 1XQ, UK, e-mail: {safak.bayram,stuart.galloway}@strath.ac.uk. Part of the work appeared in [1] at IEEE 56th International Universities Power Engineering Conference, UK, 2021.

I. Introduction

Managing electric vehicle demand at public charging facilities requires understanding of the scale and importance of the problem; the impacts of cold temperatures on EV batteries and charging process; and how the EV demand can be controlled via pricing schemes to avoid peak load. The next three subsections elaborate and address the aforementioned issues in detail.

A. Background

Road transport is one of the most carbon-emitting and energy-intensive sectors of the global economy. To achieve net-zero carbon emissions in this sector the transition towards electric vehicles (EVs) is occurring at an increased pace [2]. It has been well-documented that EVs offer significant societal benefits, such as climate change mitigation and improvement of urban air-quality [3]. Furthermore, groups of EVs could support power systems operations through the provision of ancillary services [4] and enable higher shares of renewable penetration by smoothing solar duck curves [5] and reducing wind curtailment [6].

To facilitate higher EV adoption a number of countries including the UK, EU, and the USA have introduced bold time-bound strategies to reach net-zero in the transport sector [7]. For instance, more than twenty countries including Norway, Netherlands, and UK have introduced plans to phase out sale of new petrol and diesel vehicles or have electrification plans [3]. More specifically, in support of net-zero targets the UK government aims to achieve 10 million EVs on the road by 2030 and internationally, global sales are expected to reach 230 million by the end of this decade. Furthermore, major car manufacturers such as Ford, Volvo, and General Motors have recently signed the Glasgow Declaration on Zero Emission Cars and Vans at the United Nations Climate Change Conference'21 (COP26) to manufacture only low carbon vehicles by 2035 [8].

Convenient and affordable access to public charging stations is increasingly becoming important as EVs scale up. EV infrastructure planning is often referred to as a "chicken-and-egg" problem: drivers are reluctant to switch to electric transportation if the charging infrastructure is not sufficient, but the private sector is hesitant to invest in the infrastructure if charging stations are underutilized and not profitable [9]. Therefore, initial phases of charging infrastructure deployment are usually supported by public funds to boost customer confidence and unlock environmental benefits.

Even though there has been a rapid decline in cost of lithium-ion batteries by more than 80% over the last decade, the EV market still accounts for roughly one percent of all vehicles due to compounded impacts of range anxiety, cost and long charging durations [10]. DC fast charging stations are designed to compete against petrol stations and primarily used to extend EV driving ranges in short duration [11]. Field studies further show that annually driven electric miles could increase by more than one fourth in areas where fast charging is available [10]. The role of public fast charging is even more critical in countries like Japan, China, and Singapore where the share of multi-dwelling buildings is significantly higher than detached units and fast charging is the only option for EV owners.

A recent study presented in [12] shows that one fifth of EV owners in California have switched back to combustion vehicles due to dissatisfaction with the charging infrastructure. On the other hand, a scaled and transformational

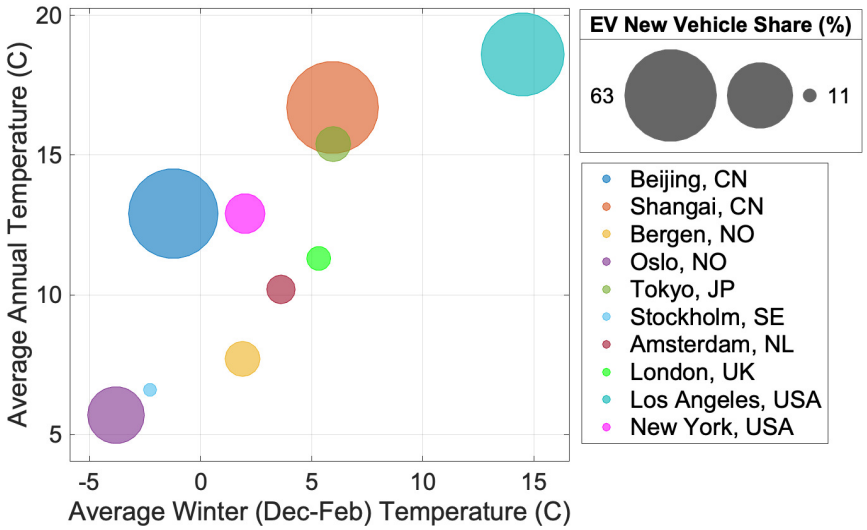

Fig. 1: An overview of average winter and annual temperatures in selected cities with high EV penetrations [17].

change towards electric transportation is beyond a technical challenge, but also includes economic and behavioural challenges. Electric vehicles will be fuelled by electrical power grids which are ageing and require significant network reinforcements to support EV charging. Economic incentives and dynamic pricing schemes are needed to control and coordinate EV demand to protect the overloading of limited grid resources, particularly during network congestion periods [13]. Moreover, recent field trials reveal that the vast majority of EV drivers charge their vehicles whenever possible due to range anxiety [14]. Hence, pricing mechanisms are needed to alter driver behaviour to eliminate unnecessary EV charging.

B. Temperature Effects on EVs

The dominant energy storage technology for the electric vehicle industry is lithium-ion batteries due to their various desired characteristics, such as high operating voltage, low self-discharge, and high-energy density [15]. EV batteries, on the other hand, are designed to operate under mild weather conditions (e.g., 21 °C) and their performance drastically reduce under cold temperatures [16]. More specifically, at low temperatures the internal resistance of the battery increases which can lead to anode lithium plating and reduced battery life cycle. None of the current EV models allow fast charging in cold temperatures [10].

Operation under cold weather creates safety issues due to short circuits and thermal runaway. To maintain safety, battery thermal management system (BTMS) uses a portion of the stored energy is used to preheat the batteries to main their performance and safety. Therefore, EV driving ranges significantly reduce due to the additional need for battery and cabin heating. Based on empirical data presented in [2], at 0°C the driving ranges of sedan EVs (e.g. Nissan Leaf, BWM i3, etc.) reduce by nearly 45% when compared to maximum range under ideal conditions. One of the challenges with preheating is the fact that it takes tens of minutes (35-40 min) to reach desired operating temperatures [15]. Unless the EV is preheated before arriving to a fast charging station (e.g. driving long distances

on highways), the charging power will be limited by BTMS and will be lower than the rated power (e.g. 50 kW for typical fast chargers [18]). Therefore, depending on the temperatures, EVs will be charged at different rates which will have implications on the charging station operations. According to Nissan Leaf's owner manual, the battery can be charged to 80% in 20 minutes at room temperature, but would take more than 90 minutes to charge at the same amount at low temperatures [10]. It is noteworthy that even if a wide fast charging network is deployed, drivers may not enjoy high charging rates. According to [19], the battery life cycle exponential drops with temperature; even at a temperature of 10 °C, the cell life is only about half of that at 25 °C. It is noteworthy that EV charging under cold weather could be an issue at major economies. For instance, 47 out of 50 US states have an average temperature lower than 10 °C in winter and the annually averaged temperatures in 23 states are below 10 °C. An overview of average winter and annual temperatures in selected cities around the world with high EV penetrations is presented in Figure 1. It can be seen that most of the cities with high EV penetration experience low winter temperatures.

Norway is another country with cold weather and high EV penetration. In [20], Norwegian EV drivers' charging behaviour at fast charging stations (CCS/Chademo 50 kW connection) is presented. As shown in Table I, annual charging power, energy, and charging durations significantly vary. For instance, half of the customers receive 31 kW or less while, only 20% of the EVs are charged with 40 kW or more. [20] further presents a seasonal analysis on EV charging and shows that charging power reduces in winter months.

Over the last years, a growing number of empirical studies were carried out to investigate the impacts of cold weather on EV battery performance and driving ranges. In [21], a simulation study is presented to quantify the amount of energy used for cabin heating in cold weather (0 °C). The results show that driving range could decrease by 40% when the cabin is heated up to 20 °C. In an empirical study presented in [22], driving range measurements were taken from two Nissan Leaf cars in Winnipeg, Canada. The analysis shows that driving range of Nissan Leaf could reduce by 70% under -26 °C weather. In [2], energy consumption and range reduction of actual EVs are presented based on data published in [23]. As shown in Fig. 2, significant amount of driving range is lost even at 0 °C. Therefore, EVs located in countries experiencing mild winter are likely to have additional EV demand due to more often EV charging.

To maintain safety and health of the battery, fast EV charging rates are limited by BTMS [22]. The relationship between charge rate and temperature was investigated and presented in [24]. In this work, authors analyse fast charging of Nissan Leaf EVs that were used in New York City as a part of the taxi fleet. EVs were charged with standard 50 kW DC fast chargers. The analysis show that the charging rate reduces by 50% under 0°C and takes about two times longer than the optimum case with 21°C. Here, the temperature is assumed to be constant during a single charging event, as it is very unlikely for the ambient temperature to change significantly. In line with this finding, this paper makes the same assumption and assumes constant temperature during charging. During the charging process, the battery temperature changes due to internal heat generation. Ultimately, increased temperature impacts the charging process, particularly for fast (50 kW) and extreme fast charging (150+ kW) cases [25]. The generated heat has two main components, namely Joule heat and reaction heat. Joule heat occurs due to the current flowing through the battery's internal resistance, which is higher at lower temperatures. Reaction heat occurs inside

TABLE I: Fast charging statistics in Norway (Q1 2016 — Q1 2018) Reference: [20].

Parameter	Average	20th Percentile	Median	80th Percentile
Energy (kWh)	9.6	4	8	13
Time (Min)	20.5	10	18	28
Power (kW)	30.2	20	31	40

the battery due to chemical reactions and increases the generated heat. Note that Joule heat is dissipated and lost during charging.

For warmer climates, fast charging also introduces additional heating on the battery. For instance, [26] shows that fast charging could increase maximum battery temperature by more than 43% in Seattle climate and more than 33% in Phoenix climate. To tackle the overheating issue, EV battery management systems employ various active and passive cooling strategies to lower the battery heating. For the cold weather charging, on the other hand, there are different external and internal preheating methods. Some of the most popular applications that are used in the EV market include air- and liquid-based preheating [15]. According to a measurement-based study presented in [15], air preheating rates hover between 0.69 °C/min to 2.33 °C/min.

Other groups of related studies are on managing EV load at charging facilities to alleviate negative impacts of concurrent EV charging. Even though the impacts of EVs on power networks (e.g. voltage drops, transformer ageing) have been well-documented in the literature (see [27] and [28]), existing studies do not consider the impacts of fast EV charging under cold weather. According to our recent survey [29], fast charging under cold weather increases harmonics, thereby the number of EVs that can be simultaneously charged is reduced to comply with IEC61000-3-12 standards. Recently, the impacts of cold weather EV charging was report in [2] and [1]. In [2], Monte Carlo based simulation was conducted to quantify the amount of extra energy needed during winter months in the UK. It was shown that more than 630 MW of peak demand would be needed in cold days if there are 10 million EVs on the road. In [1], a capacity optimisation framework is presented to calculate minimum station capacity to meet certain LoLP goals for each customer class. It is noted that the vast majority of the existing works on weather-EV charging impacts are limited to materials science/chemistry or power electronics disciplines, and the present paper is one of the first studies that proposes EV load management by considering cold weather impacts.

C. *Pricing Methods*

Devising pricing schemes for economics services furnishes a vision for design and operation of the EV charging facilities. One of the primary goals of pricing mechanisms is to recover the cost of service and sustain continued business operation [30]. However, pricing further determines how resources are used and helps station operators to reduce congestions and possibly provide demand flexibility needed for power system operators. In traditional power systems planning, over provisioning of system resources is a common practice. In this approach, the supporting network equipment would be planned according to peak load demand (number of chargers times rated power of each charger).

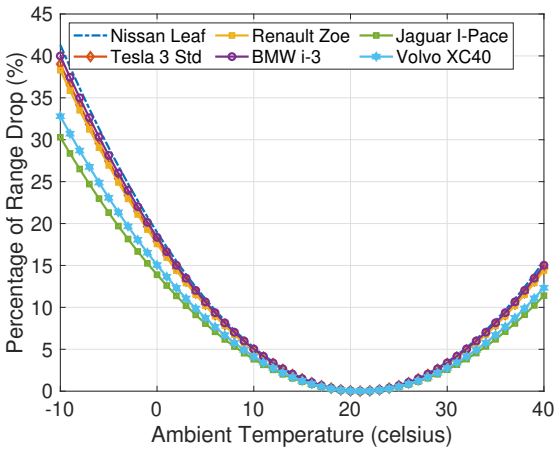

Fig. 2: EV driving ranges respect temperature [2], [23]

However, the probability of all chargers to be in use is typically very low, and even if there is congestion, the pricing methods could be used to influence drivers, coordinate service request rates and control the admission of the costumers to the stations. In this way the infrastructure requirements (e.g. MV/LV transformer, etc.) would be significantly lower than the traditional case. For instance, Ref [31] shows the trade-off between transformer capacity and the percentage of demand met in a large parking lot with smart charging. The analysis shows that meaningful reductions in the transformer size can be achieved if a small portion of the demand is not satisfied. A holistic design for charging stations, as presented in this paper, requires striking a balance between the costs associated with over provisioning (station capacity) and control.

Pricing-based control of electric vehicle demand has been reported in a growing body of literature [13], [32]–[35]. The overarching aim of the pricing schemes is to unlock EV demand flexibility to reduce network congestions and optionally support renewable energy integration [13]. In [32], pricing and routing mechanisms for differentiated charging services in an electric vehicle charging network is presented. Both social welfare and profit maximisation problems were solved by designing optimal pricing-routing policies to manage spatio-temporal EV load. In [33], scheduling of EV charging to maximise social welfare based is presented. Time varying prices are considered to minimise congestion cost. In [34], a charging station management algorithm is proposed to jointly optimise prices for EV charging, scheduling of EVs, and dropping reserved EVs. In [35], a myopic pricing policy is developed to coordinate EV charging among geographically distributed charging stations.

In [36], the authors present a framework that jointly optimizes pricing, scheduling and admission control for EV charging stations using a tandem queueing model. It is similar to the approach presented in [36] which employs convex utility functions and aims to maximize social welfare. In [37], the authors presented an M/M/c queue based charging station model which accepts AC and DC charging. In this model, the waiting space for the station is assumed to be large and when the waiting times to get service are lower than a certain threshold, flat pricing is applied. However, as the station load increases, scheduled pricing policy is applied to lower demand. From a related modelling standpoint, in [38], M/M/K/K queue (single-class loss model) is used to model a charging station that

provides multiservice (vehicle to grid, battery swapping etc.) to customers. A detailed review of the pricing methods is presented in [13] which further provides examples on utility functions for EV charging and pricing methods used in the literature.

Note that existing multi-class models rely on separate queues and tackle a fixed number of customer classes. The model presented in this paper is widely applicable and can support the modelling of an arbitrary number of customer classes. Hence, the proposed model can be expanded to different applications, such as ultra-fast charging hubs designed to serve both EVs and medium and high duty vehicles.

D. *Contributions*

Fast charging stations located in cold climates inherently provide different charging service depending on the battery temperatures. Existing literature on EV-grid load management and grid-integration assumes that EVs operate under optimum driving conditions and charged at rated capacity. Moreover, pricing based multi-class EV charging studies only consider different charging types (e.g. level 1 and 2) and are typically limited to two classes. However, charging under cold weather conditions this requires modelling and optimisation of higher number of customer types and their interactions with the station resources. Recall that EV penetration is very high in regions with long and cold winter months (Northern Europe, Parts of China, and Northern USA), the investigation of cold weather on EV charging patterns and controlling its impacts on the power grid is a critical problem. Moreover, current pricing tariffs for public fast charging stations are based on the time or the session [13], which creates concerns about fairness as the drivers with cold batteries are required to pay more than the customers with warmer batteries. To that end, the contributions of this paper are as follows:

- a geographically distributed stochastic charging station model based on a multidimensional loss system is proposed. The charging station serves multi-class EV drivers, which are classified based on ambient temperature and associated charging power.
- a pricing-based load control framework to match time-varying grid resources with customer demand is developed. Efficient calculation of loss of load probabilities (event that instantaneous demand is higher than supply) for each customer class is shown, which creates the basis of the proposed framework.
- a demand control framework is formulated as a social welfare optimisation problem and provide a convex optimisation formulation to compute unique congestion prices (plug-in fees) that are used to determine the optimal arrival rates.
- A number of case studies are designed to explain the relationship between different system parameters such as station capacity (kW), EV arrival rates (number of EVs per hour), and prices for each EV class. The results show that the prices are commensurate with their contribution to network congestion.

II. System Description

A. *Overview*

EV charging demand at fast charging facilities are mainly determined by the customer's needs, preferences, and technological constraints. Basic customer needs include the amount of energy needed (in kWh), while the

preference includes the amount of service time that drivers are willing to spend. Moreover, the ambient and the battery temperature determine the rate at which EVs can be charged. Hence, EVs requesting service under cold weather are naturally grouped into multiple customer classes, which are defined by the preceding attributes. Based on this premise, the charging station operations rely on the economic interaction between the customers and the network operators.

More specifically, this framework proposes a pricing-based load management system for fast charging networks located in urban areas with high EV population. The primary objective is to set prices for charging service for each customer class to maximise social welfare. For the station network operator, a pricing mechanism reduces network overloading that is defined by the loss of load probability, i.e. the probability that the demand exceeds supply. Moreover, customers who are charged with lower power due to cold ambient temperatures are offered lower prices as their contribution to congestion is lower than the other customers with high charging power.

B. Charging Network Model

The charging network is composed of N charging stations which are located in a well-confined region and supplied by the same distribution substation. The network serves J distinct customer classes. Let j denote the customer class index, which takes values between 1 and J. EVs in class j are charged with b_j kW and the charging durations are assumed to be exponentially distributed with rate μ_j. For instance, if $\mu_j = 2$, then on average, two EVs are charged in one hour. Charging rates b_j for $j \in \{1, .., J\}$ are determined by the temperature of the battery and assumed to be constant throughout the charging session, as documented by the empirical study given in [24].

As the load on the network varies over time, e.g. the headroom in the supporting substations, the amount of electrical power that can be used to charge EVs varies over time. Therefore, the network is a dynamic system with time index $t \in \mathbb{T}$ in which C_t represents the total headroom available at time t and assumed to be constant during any given time index t. It is important to note that when the instantaneous load on the station is more than the station capacity, an outage even occurs. Therefore, the probability of an outage, or loss of load probability (LoLP) denoted by β_j for class j, naturally serves as a performance metric [39].

Controlling EV demand is a critical for charging network operators as high EV demand could increase outage events and unwanted service disruptions lead to network reinforcement cost. Pricing schemes for admission control enables network operators to influence EV charge decisions to reduce outage events to keep LoLP at reasonable levels (e.g. below 5%). Let $p_j(t)$ denote the prices of charging service for type j and the price vector $\boldsymbol{p}(t) \triangleq [p_1(t), \ldots, p_J(t)]$ denotes prices for each customer type. Based on the prices, EVs decide to request service or decide to defer charging. Let $\lambda_j^n(t; \boldsymbol{p}(t))$ denote that charging request rate at station $n \in \{1, .., N\}$ during period t. Then, the aggregate arrival rate of EVs of class j is

$$\lambda_j(t; \boldsymbol{p}(t)) \triangleq \sum_{n=1}^{N} \lambda_j^n(t; \boldsymbol{p}(t)) \ . \tag{1}$$

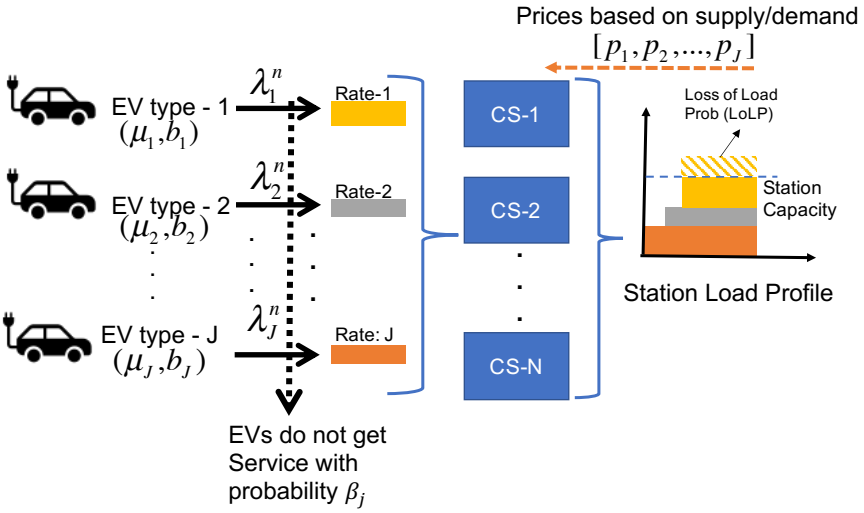

Fig. 3: Schematic overview of the proposed system.

It is noteworthy that the arrival rates are assumed to follow a Poisson process as documented literature [39]–[41]. Moreover, the arrival rate vectors are defined as follows

$$\boldsymbol{\lambda}^n(t;\boldsymbol{p}(t)) \triangleq [\lambda_1^n(t;\boldsymbol{p}(t)),\ldots,\lambda_J^n(t;\boldsymbol{p}(t))] , \tag{2}$$

and

$$\boldsymbol{\lambda}(t;\boldsymbol{p}(t)) \triangleq [\lambda_1(t;\boldsymbol{p}(t)),\ldots,\lambda_J(t;\boldsymbol{p}(t))] . \tag{3}$$

Further note that LoLP defined above is a function of the arrival rates and prices. Therefore, let $\beta_j(t;\boldsymbol{\lambda}(t;\boldsymbol{p}(t))$ denote the probability that customers of class j are "blocked" and $\boldsymbol{\beta}(t;\boldsymbol{\lambda}(t;\boldsymbol{p}(t))$ denote the corresponding LoLP vector. The system model is shown in Figure 3. For ease of representation, the explicit dependence on t is omitted in the rest of the paper.

C. Pricing-based Control

The main goal of the control framework is to leverage pricing to shape EV arrival rates of each type so that network operators can provide service with low levels of service interruptions. More specifically, the goal is to devise a distributed control framework to maximise social welfare or aggregate utility, which necessitates EV arrivals of each customer type to follow optimal rates. At each station n, the utility is a function of arrival rates $\boldsymbol{\lambda}$ and LoLPs $\boldsymbol{\beta}(\boldsymbol{\lambda})$, that is

$$U^n(\boldsymbol{\lambda}^n;\boldsymbol{\beta}(\boldsymbol{\lambda})) \tag{4}$$

Then, the social welfare or the aggregate utility of the entire network is the sum of all utilities, that is

$$W = \sum_{n=1}^{N} U^n(\boldsymbol{\lambda}^n;\boldsymbol{\beta}(\boldsymbol{\lambda})) . \tag{5}$$

Hence, the social welfare problem aims to maximise the aggregate utility W over all combinations of the arrival rates $\{\boldsymbol{\lambda}^n\}_{n=1}^N$, that is,

$$\max_{\{\boldsymbol{\lambda}^1,\ldots,\boldsymbol{\lambda}^N\}} \sum_{n=1}^{N} U^n(\boldsymbol{\lambda}^n; \boldsymbol{\beta}(\boldsymbol{\lambda})) \ . \tag{6}$$

It is further assumed that the utility function U^n, is decreasing in the LoLPs β_j and increasing in the arrival rates $\{\lambda_j\}$. Moreover, it is assumed that U^n is concave in λ_j and continuously differentiable in all of its parameters [39].

D. Global Optimisation Problem

This section presents the formulations related to the global social welfare optimisation problem given in (6) and shows that the solution method is amenable to distributed implementation. More specifically, the EV arrival rates are dynamically adjusted based on the prices announced by the station operator and distributed adjustment of EV demand leads to a socially optimal welfare for the entire network.

Note that each station's utility function U^n is concave in λ_j, decreasing in the LoLP β_j, and continuously differentiable in all of its arguments. The social welfare $W = \sum_{n=1}^{N} U^n$ is maximised when $\forall n \in \{1,\ldots,N\}$ and $\forall j \in \{1,\ldots,J\}$

$$\frac{\partial W}{\partial \lambda_j^n} = \frac{\partial U^n}{\partial \lambda_j^n} + \sum_{l=1}^{N}\sum_{s=1}^{J} \frac{\partial U^l}{\partial \beta_s} \cdot \frac{\partial \beta_s}{\partial \lambda_j^n} = 0 \ . \tag{7}$$

Since the LoLP of each charge type depends only on the sum of the arrival rates of that type $\lambda_j = \sum_{n=1}^{N} \lambda_j^n$, from (7) the following expression is found $\forall n \in \{1,\ldots,N\}$ and $\forall j \in \{1,\ldots,J\}$:

$$\frac{\partial W}{\partial \lambda_j^n} = \frac{\partial U^n}{\partial \lambda_j^n} + \sum_{l=1}^{N}\sum_{s=1}^{J} \frac{\partial U^l}{\partial \beta_s} \cdot \frac{\partial \beta_s}{\partial \lambda_j} = 0 \ . \tag{8}$$

Solving (8) gives a *globally* optimal arrival rates for each customer class.

E. Local Optimisation Problem

The *local* optimisation problem further includes the prices p_j and has the following form for each station $n \in \{1,\ldots,N\}$ and customer type $j \in \{1,\ldots,J\}$

$$\tilde{U}^n(\boldsymbol{\lambda}^n; \boldsymbol{\beta}(\boldsymbol{\lambda})) \ \triangleq \ \underbrace{U^n(\boldsymbol{\lambda}^n; \boldsymbol{\beta}(\boldsymbol{\lambda}))}_{\text{gain}} \ - \ \underbrace{\sum_{l=1}^{J} p_l \lambda_l^n (1-\beta_l)}_{\text{cost}} \ . \tag{9}$$

By solving the local optimisation problem given in (9), the optimal arrival rates at the station n is computed as $\boldsymbol{\lambda}^n = [\lambda_1^n, \ldots, \lambda_J^n]$. Using the convexity of the problem, the locally optimal arrival rates further satisfy:

$$\frac{\partial U^n}{\partial \lambda_j^n} - p_j(1-\beta_j) = 0 \ . \tag{10}$$

Based on the announced prices, each station n can compute its own optimal arrivals by solving (10). It is noteworthy that individual EVs do not have information about the derivatives of arrival rates with respect to β_j as this leads to local optimisation problem [42]. Moreover, the size of the system is assumed to be large enough such that individual EVs do not impact LoLP.

F. Connection between Local and Global Problems

The connection between local and global optimisation problems is related to prices. By comparing global optimisation problem given (8) and local optimisation problem given in (10), it can be deduced that the optimal prices for $j \in \{1, \ldots, J\}$ satisfy:

$$p_j^* = -(1-\beta^j)^{-1} \sum_{l=1}^{N} \sum_{s=1}^{J} \frac{\partial U^l}{\partial \beta^s} \cdot \frac{\partial \beta^s}{\partial \lambda_j} \ . \tag{11}$$

When price p_j^* is offered to customer of type j, the solution of local optimisation problem in (9) satisfies the conditions given in (7) and guarantees the global optimisation problem given in (8) as established in [42]. Therefore, the local solutions become the equilibrium point, since no single customer has incentives to deviate from its locally optimal solution. Hence, optimal prices $\{p_1^*, p_2^*, \ldots, p_J^*\}$ can be considered as congestion prices, as each customer pays others for 1 unit of marginal decrease in their utility due to an increase in the LoLP. To calculate optimal prices, both the utility functions and the derivatives of the LoLP in respect to arrival rates need to be explicitly known.

G. Alternative Approaches

It is important to note that the proposed pricing-based control method can be interpreted from a game theoretic perspective. As one approach, the distributed control framework can be modelled as a Stackelberg (leader-follower) game in which the charge point operator acts as the leader who commits to a strategy before followers (multiple classes of EVs) can pick their strategy (a detailed analysis of such games is presented in [43]). The game in its strategic form is defined as

$$\Gamma = \{\{\mathcal{N} \cup \mathcal{J}\}, \{\boldsymbol{p}_j\}, \{X_{j\in\mathcal{J}}\}, \{U_{n\in\mathcal{N}}\}, \{U_{j\in\mathcal{J}}\}\},$$

where $\mathcal{N}$=$\{1, 2, \cdots, N\}$ is the set of charging stations and $\mathcal{J}$=$\{1, 2, \cdots, J\}$ the set of EV groups of a specific group that request charging service. The leader's strategy is to set prices for each customer type and represented by a vector $\{\boldsymbol{p}_j\}$, while the strategy of the followers, $X_{j\in\mathcal{J}}$, is to choose arrival rates $\boldsymbol{\lambda}^n$. Here both the leader and the followers have convex utility functions, as given in (4) and (9) respectively. The optimal solution in the preceding game is the case where each player lacks any incentive to change their initial strategy. Therefore, the analysis given above shows that the optimal prices given in (11) leads to the Nash equilibrium. Due to page limitations, the analysis for obtaining Nash equilibrium is not included in this paper and instead [44] could be referred to as a main source for this derivation.

III. Computation of Loss-of-Load Probabilities and Associated Derivatives

A. Motivating Example

The pricing-based control framework discussed above requires computation of LoLPs (β_j, $\forall j$) and derivatives respect arrival rates ($\frac{\partial \beta^s}{\partial \lambda_j}$, as given in (11)). The system described above falls under multi-dimensional Erlang loss systems (see [45], [46]). In such systems, a newly arriving customer requesting a certain amount of resources is either admitted to the station or is "blocked" and leaves the system. To illustrate the described system, an example

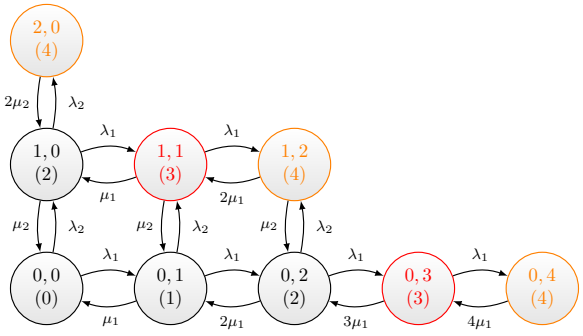

Fig. 4: Sample Markov chain model for two class customers with station capacity $C = 4$, $b_1 = 1$, $b_2 = 2$. Each state is represented by the number of class 1 and class 2 EVs. The number given in parentheses shows the amount of resources in use.

is presented in Fig. 4 which shows the Markov chain model for a two class system with arrival and charging states denoted by (λ_1, λ_2) and (μ_1, μ_2). The station has a capacity of 4 units ($C = 4$) and demand beyond this capacity will not be served (outage event). Customers in first class request $b_1 = 1$ unit of resources, while customers in the second class are charged two times faster ($b_2 = 2$). As shown in Fig. 4, the system state is described with two parameters: number of EVs from class 2 and class 1. Moreover, the number shown in parentheses reflects the amount of resources in use. For instance, at state $(1, 2)$ there is one EV from class 2, two EVs from class 1, and three (out of four) amount of resources are in use. To that end, the states shown in orange are "blocking" states for class 1 customers, as an arriving customer will not be served due to shortage of resources. Similarly, orange and red states are "blocking" states for class 2 customers, as an arriving customer finds resources less than $b_2 = 2$. Steady state probability distributions and LoLP for each customer class can be calculated by solving

$$\pi \boldsymbol{M} = \mathbf{0} \quad \text{and} \quad \sum_{s=1}^{S} \pi_i = 1 \ , \tag{12}$$

where S is the number of states and equal to 9, π is the vector of steady state probabilities and M is the infinitesimal generator matrix [47]. Specifically, elements of the matrix represented by column index k and row index l can be written as

$$m_{kl} \geq 0 \ , \quad \forall k \neq l \quad \text{and} \quad m_{kk} = -\sum_{k \neq l} m_{kl} \ , \quad \forall k \ . \tag{13}$$

Notice that (12) contains S unknown parameters and $S + 1$ equations can be with Gaussian elimination. For the case study (12) can be constructed as follows: Let S_i denote the state number from, $i = 1, 2, ..., S$, where S_1 corresponds to state $(0, 0)$, and S_9 corresponds to $(2, 0)$. Moreover, let λ_T and μ_T denote the sum of individual arrival and service rates, i.e. $\lambda_T = \lambda_1 + \lambda_2$ and $\mu_T = \mu_1 + \mu_2$. Then the matrix M for the two class example becomes:

$$M = \begin{array}{c} \\ S_1 \\ S_2 \\ S_3 \\ S_4 \\ S_5 \\ S_6 \\ S_7 \\ S_8 \\ S_9 \end{array} \begin{array}{c} \begin{array}{ccccccccc} S_1 & S_2 & S_3 & S_4 & S_5 & S_6 & S_7 & S_8 & S_9 \end{array} \\ \begin{pmatrix} -(\lambda_T) & \lambda_1 & 0 & 0 & 0 & \lambda_2 & 0 & 0 & 0 \\ \mu_1 & -(\mu_1+\lambda_T) & \lambda_1 & 0 & 0 & 0 & \lambda_2 & 0 & 0 \\ 0 & 2\mu_1 & -(2\mu_1+\lambda_T) & \lambda_1 & 0 & 0 & 0 & \lambda_2 & 0 \\ 0 & 0 & 3\mu_1 & -(3\mu_1+\lambda_1) & \lambda_1 & 0 & 0 & 0 & 0 \\ 0 & 0 & 0 & 4\mu_1 & -4\mu_1 & 0 & 0 & 0 & 0 \\ \mu_2 & 0 & 0 & 0 & 0 & -(\lambda_T+\mu_2) & \lambda_1 & 0 & \lambda_2 \\ 0 & \mu_2 & 0 & 0 & 0 & \mu_1 & -(\lambda_1+\mu_T) & \lambda_1 & 0 \\ 0 & 0 & \mu_2 & 0 & 0 & 0 & 2\mu_1 & -(\mu_1+\mu_T) & 0 \\ 0 & 0 & 0 & 0 & 0 & 2\mu_2 & 0 & 0 & -2\mu_2 \end{pmatrix} \end{array}$$

As a case study, it is assumed that $\lambda_1 = \lambda_2 = 1$ (EVs/hour) and the charging rates are chosen as $\mu_1 = \mu_2 = 2$.. Then, solving (12) yields to

$$\pi = [0.3920\ 0.1684\ 0.0388\ 0.0065\ 0.0008\ 0.2236\ 0.0633\ 0.0128\ 0.0939].$$

LoLP for class 1, denoted by β_1, can be calculated by summing the probability of states shown in orange, that is $\beta_1 = 0.0008 + 0.0128 + 0.0939 = 0.1075$. Similarly, β_2 is the sum of probability of states shown in orange and red which is $\beta_2 = 0.1773$. Note that as the number of states grows, M matrix grows significantly. Therefore, this method becomes computationally expensive quite quickly and a more efficient calculation method is presented in the next section.

B. Mathematical Formulations

To compute the probability of such events, J independent time reversible continuous time Markov chains are analysed as follows. The system state is defined by the number of EVs of each type, i.e., $\boldsymbol{Q} \triangleq [Q_C^1, Q_C^2, \ldots, Q_C^J]$ for a given station capacity C and the state space is given by $\Omega \triangleq \{\boldsymbol{Q} : \sum_{j=1}^{J} b_j Q_\infty^j \leq C\}$. It is important to note that the present analysis first assumes that the charging station has infinite capacity, therefore states represented by Q_∞, and then the probability distributions will be conditioned in respect to finite capacity case. The rationale behind this approach is that the closed form expressions for the infinite case exists and can be used to derive the finite capacity case. Note that due to Poisson arrival process assumption, mean, and variance of Q_∞ become $\mathbb{E}\left[Q_\infty^j\right]$ = var $\left[Q_\infty^j\right]$ = $q_j = \frac{\lambda_j}{\mu_j}$.

Let $\tilde{Q}_C^j$ represent the highest number of EVs of type j that can be charged simultaneously. By ranking the charging rates in descending order $b_1 \geq b_2 \geq \cdots \geq b_J \geq 0$, the maximum number of EVs of each type that can be in the system has the following relation; $0 \leq \tilde{Q}_C^1 \leq \tilde{Q}_C^2 \leq \cdots \leq \tilde{Q}_C^J$. Then the probability of being at an arbitrary state $\boldsymbol{Q}$ can be written as [48]:

$$\overline{\pi}(\mathbf{Q}) = \prod_{j=1}^{J} \frac{q_j^{Q_\infty^j}}{Q_\infty^j!} e^{-q_j} \ , \tag{14}$$

where Q_{∞}^{j} denote the number of EVs of class j simultaneously requesting b_j units of power. By conditioning on a finite capacity, a generic system state $\boldsymbol{Q}$ can be calculated as

$$\pi(\boldsymbol{Q}) = \frac{\overline{\pi}(\mathbf{Q})}{\sum_{\tilde{Q}\in\Omega}\overline{\pi}(\tilde{\mathbf{Q}})}. \tag{15}$$

To calculate LoLP, the related system states for customer type j can be defined as

$$\Psi_j = \{\boldsymbol{Q} : C - b_j \ < \ \sum_{k=1}^{J} b_k Q_C^k \ \leq \ C\} \ .$$

It is noted that Ψ_1 corresponds to orange states in the presented two class example (see Fig. 4). Then, LoLP can be re-written as:

$$\beta^j(\boldsymbol{q}, \boldsymbol{b}) = \sum_{s\in\Psi_j}\pi(s) = 1 - \sum_{s\notin\Psi_j}\pi(s) \ . \tag{16}$$

In (16), the second term denotes the probability that station falls below $C - b_j$ (instead of C) and $\pi(s)$ represents the steady state probability distribution. Moreover, let us define the function $R(C, J)$ as

$$R(C,J) \triangleq \sum_{\{\boldsymbol{Q}:\ \boldsymbol{bQ}\ \leq\ C\}} \prod_{j=1}^{J} \frac{q_j^{Q^j}}{Q^j!} \ , \tag{17}$$

which is used to compute LoLP for each class j as:

$$\beta_j(\boldsymbol{q}, \boldsymbol{b}) = 1 - \frac{R(C - b_j, J)}{R(C, J)}. \tag{18}$$

Note that set $\{\boldsymbol{Q} : \ \boldsymbol{bQ} \ \leq \ C\}$ in (17) hosts all system states that correspond to zero outage events. Even though (18) present an explicit representation for β_j, actual computation could be costly as typical station sizes could be in Mega-watt levels with 3-5 different classes. Therefore, LoLP computations are carried out with the Kaufman-Roberts algorithm (Algorithm 1) which involves a simple recursion (as documented in [49]) Let c represent the total amount of resources being in use and

$$\alpha(c) \ \triangleq \ \mathrm{Prob}\{\text{c units of power in use}\} \ .$$

Then, the function $\alpha(c)$ becomes

$$\alpha(c) = \sum_{\{\boldsymbol{Q}:\ \boldsymbol{bQ}\ \leq\ c\}} \frac{q_j^{Q^j}}{Q^j} \cdot \frac{1}{R(C,J)} \ , \tag{19}$$

and the corresponding LoLP for type j can be computed by solving

$$\beta_j(\boldsymbol{q}, \boldsymbol{b}) = \sum_{i=0}^{b_j - 1} \alpha(C - i) \ . \tag{20}$$

The final element in computation of optimal prices given in (11) is the derivatives of β_j with respect to customer arrival rates λ_j for each class. To calculate derivatives, convolution algorithms presented in [46] are adopted. In this approach, the derivative of LoLP associated with a customer class j with respect to traffic intensity of another class can be written as

$$\begin{aligned} \frac{\partial \beta_{j_1}}{\partial q_{j_2}} \quad &= \alpha(C - b_{j_1}) + \alpha(C - b_{j_2} - 1) + \cdots \\ &+\alpha(C - b_{j_2} - b_{j_1} - 1) - (1 - \beta^{j_2})\beta^{j_1} \ , \end{aligned} \tag{21}$$

Algorithm 1 Kaufman-Roberts Algorithm [49]

Set $\kappa(0) = 0$ and $\kappa(i) = 0$ for $i \in \mathbb{R}^-$
for i=1 to C **do**
$\kappa(i) = \frac{1}{i} \sum_{j=1}^{J} b_j q_j (j - b_j)$
end for
Compute $R = \sum_{i=1}^{C} \kappa(i)$
for i=0 to J **do**
$\alpha(i) = \frac{\kappa(i)}{R}$
end for
for j=1 to J **do**
$\beta_j(\boldsymbol{q}, \boldsymbol{b}) = \sum_{i=C-b_j+1}^{C} \alpha(i)$
end for

where $j_1 \neq j_2$ and $\alpha(\cdot)$ is given in (19). To reduce the complexity of the computations, the elasticity property is used. According to this property, the sensitivity of customer type j to customer type k is the same as the sensitivity of customer class k to class j as reported in [50]. In other words, the elasticity property reduces the number of computations needed as

$$\frac{\partial \beta_{j_1}}{\partial q_{j_2}} = \frac{\partial \beta_{j_2}}{\partial q_{j_1}} \ . \tag{22}$$

The Kaufman-Roberts algorithm presented in Algorithm 1 is a recursive algorithm and its computational complexity can be written in terms of station capacity C and the number of classes J. By considering the recursions, the algorithm has the worst-case complexity of $O(JC)$ [49]. Considering the fact that there could be 3-4 classes in a fast charging station, the algorithm would rapidly converge to calculate LoLPs [49].

IV. Case Studies

A. Motivating Example

As a first case study, a charging station serving two customer classes is presented. It is assumed that the utility function of a single station n increases with the customer arrival and decreases with prices paid to the distribution network operator and higher LoLP. To that end, a logarithmic utility function, widely used in literature [13], is adopted as:

$$U = \begin{cases} \sum_{j=1}^{J} \omega_j \log(1 + \lambda_j) - \theta_j \log(1 + \beta_C^j) - p_j \lambda_j (1 - \beta_j) & \lambda_j > 0 \\ 0 & \text{otherwise} \end{cases} , \tag{23}$$

where ω_j and θ_j are the weights of each EV class and each has the following monotonic structure $\omega_1 > \omega_2 > ... > \omega_J$ and $\theta_1 > \theta_2 > ... > \theta_J$ for $b_1 > b_2 > ... > b_J$ as customers who demand more resources leads to higher social utility.

As a first evaluation, the following parameter settings are assumed. There are two customers classes ($J = 2$) with charging power $b_1 = 50$ kW and $b_2 = 30$ kW. and service durations are set as $\mu_1 = 1.67$ and $\mu_2 = 1$ so that each vehicle receives, on average, 30 kWh of energy. Moreover, the station capacity is set as $C = 800$ kW and utility function parameters are set as $\omega_1 = 25$, $\omega_2 = 10$ and $\theta_1 = 60$, $\theta_1 = 30$. Note that this parameter setting is expanded

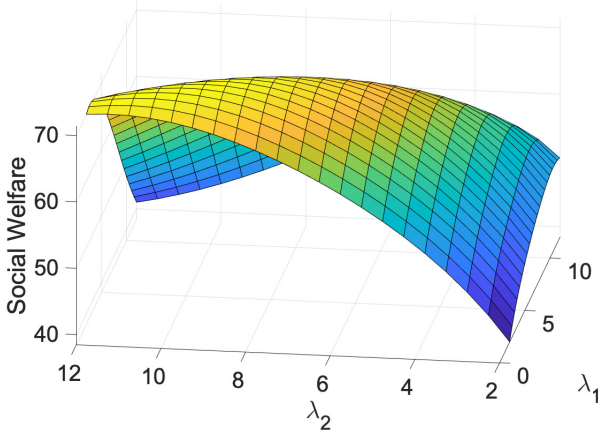

Fig. 5: Social welfare evaluation with two classes.

TABLE II: Customer classes for the case studies. In Scenario 1, each vehicle receives 30 kWh of energy. In Scenario 2, each vehicle is charged for 30 min.

Class	Scenario 1 (Equal Energy (kWh))			Scenario 2 (Equal Duration)	
	Charge Rate (kW)	Average Duration (min)	Service Rate (no of charged EVs per hour)	Average Duration (min)	Service Rate (no of charged EVs per hour)
1	50	36	1.67	36	1.67
2	40	45	1.33	36	1.67
3	30	60	1	36	1.67
4	20	90	0.66	36	1.67

to four class case and used in the next section (presented in Table II). The utility function presented in (23) is evaluated and the outcome presented in Figure 5. In this example, optimal prices are calculated as $p_1 = 0.3071$ and $p_2 = 0.2728$, optimal arrival rates are calculated as $\lambda_1 = 10.5$ and $\lambda_2 = 4.5$ and the maximum utility is attained as 71.39. Notice that the network gains more utility by accepting higher charging rate vehicles, but charges lower prices for EVs with colder batteries. Thus, if the customers do not have any motivation to deviate from the optimal case, for instance if arrival rates increase, the cost component of (9) will also increase due to higher LoLP levels. On the other hand, if customer demand is lower than the optimal case there would be a loss of gains as given in the same equation.

B. Case Study with Four Classes

In this section more comprehensive case studies are presented with EV four classes and as presented in Table II. EVs in class 1 are charged with 50 kW as their batteries are assumed to be warm enough to receive full charging rate. On the other hand, EVs in the 4th class only receive 20 kW charging rate due to cold battery temperature. The other two classes are assumed to be in between these two cases. The charging rates are determined based on measurement studies documented in [20] and [24].

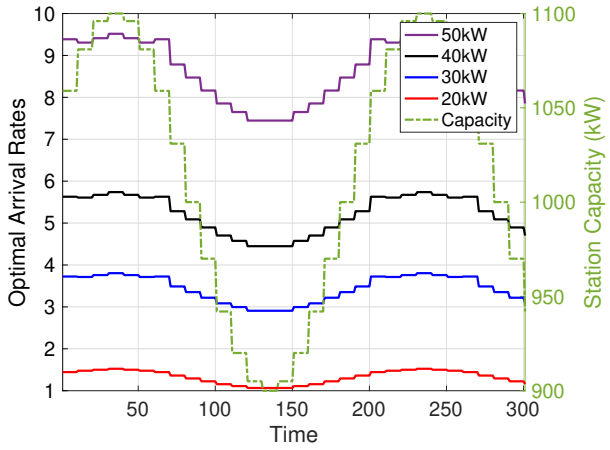

(a) Optimal Arrival Rates

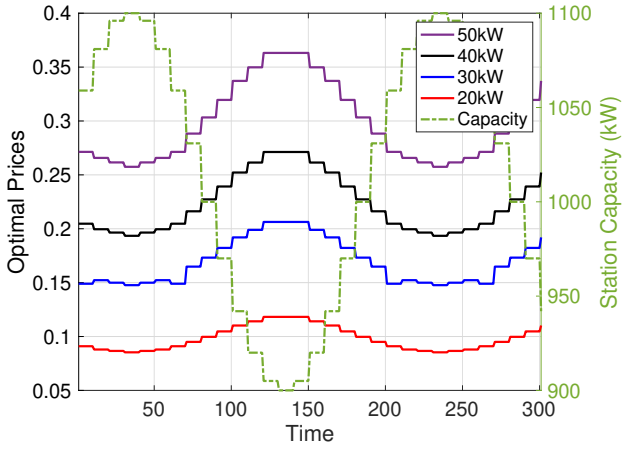

(b) Optimal Prices

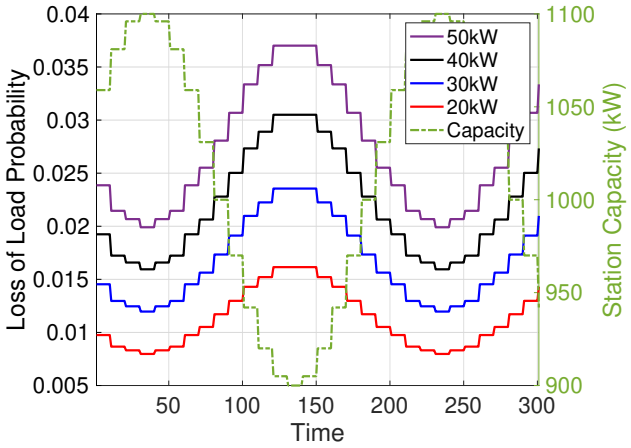

(c) Loss of Load Probability

Fig. 6: Case study-1: Each EV is charged up to 30 kWh.

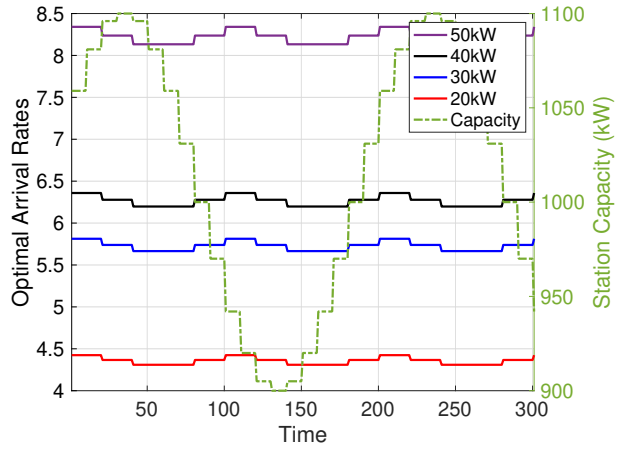

(a) Optimal Arrival Rates

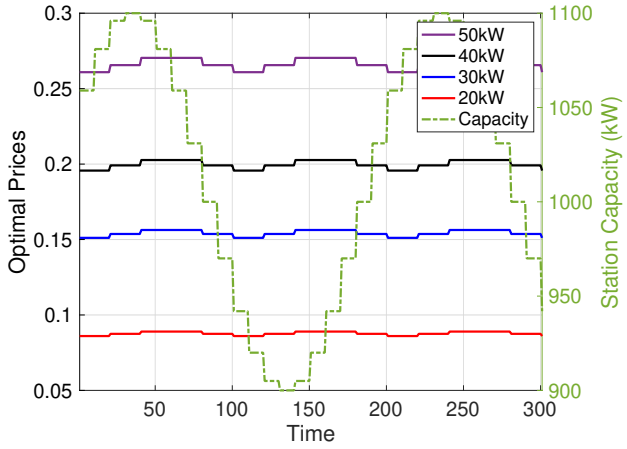

(b) Optimal Prices

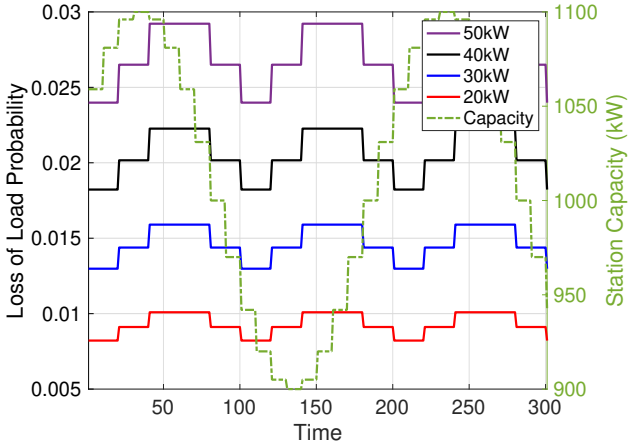

(c) Loss of Load Probability

Fig. 7: Case study-2: Each EV is charged for 30 minutes.

In the first scenario, it is assumed that each vehicle is charged 30 kWh of energy and charging durations and rates are calculated accordingly. The station capacity is assumed to follow a sinusoidal wave and set as $C(t)$=$100 + 100\sin(2\pi t/40)$ and assumed to be constant for every $T = 10$th duration. In Fig. 6, the results for the first scenario are presented. As shown in Fig. 6 (a), the station network accepts higher percentage of customers from the first class (50 kW) as customers of this class contributes to higher system-wide utility. In Fig. 6 (b), prices for each customer class are presented. It can be seen that the lowest price is requested from the fourth customer class (20 kW) as the customers in this class are the least contributors to system congestion. Moreover, as the pricing scheme is inversely proportional to station capacity and class dependent prices increase when the station capacity reduces. The last evaluation is on the computation of LoLP (β_j for each class. Note that the LoLPs are sorted as $\beta_1 > \beta_2 > \beta_3 > \beta_4$ since the charging rates follow $b_1 > b_2 > b_3 > b_4$ and the optimal arrival rates are sorted as $\lambda_1 > \lambda_2 > \lambda_3 > \lambda_4$.

In the second case study, it is assumed that an arbitrary EV spends 30 minutes in the charging station regardless of its class. In this case, the same set of parameters are computed and presented in Fig. 7. Compared to the first scenario the following observations are made. As customer classes 2, 3 and 4 spend less time in the charging station compared to the first scenario, the station accepts more customers and the optimal arrival rates increase. Secondly, prices for each class reduce as the congestion levels reduce with shorter charging durations. Therefore, fairness among different charger types are achieved as prices are determined based on the intensity of resources requested rather than equal pricing of EVs regardless of the charging rates. In both case studies, LoLPs are sorted according to the amount of resources they request. This is because when the charging rate is higher, there are more "blocking" states, as illustrated by the example given in Fig. 4.

V. Conclusion

In this paper, a stochastic charging station model that is developed for multi-class fast EV charging service was presented. The station model is based on a multi-rate loss system where each EV class is determined by ambient temperature dependent charging power. A convex optimisation problem formulation was provided to compute optimal arrival rates for each class to maximise social welfare. It was shown that optimal arrival rates can be locally computed by calculating congestion prices for each customer class. Special attention was given to computation of loss of load probabilities and their derivatives with respect to arrival rates, since they are important for overall network efficiency and constitute a key part of the proposed model. Two case studies were designed. In the first, each vehicle type was assumed to charge up to 30 kWh, hence, customers with cold batteries had to charge for longer. In the second, each vehicle type was assumed to charge for the same duration (30 min). The results show that congestion prices provide a fairer costing for plug-in fees, as EVs with cold batteries pay a lower fee commensurate with their contribution to network congestion.

It was found that the current academic literature in these areas lacks studies that investigate the relationship between ambient temperature, battery temperature, and charging power. Therefore, when modelling the charging power, it is assumed to be constant during the charging session based on the assumptions made in [24]. On the other hand, the battery temperature may slightly increase during the charging.The amount of temperature increase

depends on initial SoC charge level, initial battery temperature, ambient temperature, and the auxiliary use of energy for heating the cabin. Since the charging session is assumed to be short (15-20 min based on Table I), the amount of temperature rise is expected to be low. If datasets on this topic are made publicly available, the modelling capability could be improved by considering the average charging power during the charging session.

The modelling and optimisation frameworks presented in this paper rely on pubicly available datasets, therefore, are subject to the following limitations. First, the station model relies on exponentially distributed charging times. As given earlier in the paper, this assumption is commonly made in the literature due to lack of publicly available datasets for fast chargers. Moreover, the utilisation of existing fast chargers is still very low because most of the early EV adopters have dedicated chargers at home and use fast chargers to complement their driving ranges. Existing data-driven studies represent parking lots with level 2 chargers. To that end, larger-scale datasets collected from public fast chargers are needed to improve the modelling accuracy.

Second, it is assumed battery management system of EVs have the capability to determine battery temperature and hence the charging rate that the EV can accept is assumed to be communicated with the charging station in a truthful way. If some of the customers cheat on their submissions, the socially optimum arrival rates may not be achieved. Hence, the impacts of potential cyber attacks need to be considered as a future work. Third, players are assumed to be rational and range anxiety is not modelled. Similar to the first constraint, modelling range anxiety requires field data on initial state of charge (SoC) levels of visiting vehicles. To tackle range anxiety, EVs with high SoC levels could be offered higher prices to avoid congestion and give priority to customers who are in urgent need. This paper addresses the problems pertinent to ambient temperature impacting EV charging. Such approaches require greater attention as EVs are becoming the main mode of transport and charging infrastuctures need to be planned accordingly.

REFERENCES

[1] I. S. Bayram, "Capacity optimisation framework for fast charging stations operating under cold weather," in *2021 56th International Universities Power Engineering Conference (UPEC)*, 2021, pp. 1–6.

[2] I. Koncar, , and I. S. Bayram, "A probabilistic methodology to quantify the impacts of cold weather on electric vehicle demand: A case study in the uk," *IEEE Access*, 2021.

[3] "Global ev outlook 2021," Tech. Rep., 2021. [Online]. Available: https://www.iea.org/reports/global-ev-outlook-2021

[4] A. Ghazanfari and C. Perreault, "The path to a vehicle-to-grid future: Powering electric mobility forward," *IEEE Industrial Electronics Magazine*, 2021.

[5] R. Jovanovic, S. Bayhan, and I. S. Bayram, "A multiobjective analysis of the potential of scheduling electrical vehicle charging for flattening the duck curve," *Journal of Computational Science*, vol. 48, p. 101262, 2021.

[6] J. Dixon, W. Bukhsh, C. Edmunds, and K. Bell, "Scheduling electric vehicle charging to minimise carbon emissions and wind curtailment," *Renewable Energy*, vol. 161, pp. 1072–1091, 2020.

[7] A. Nurdiawati and F. Urban, "Towards deep decarbonisation of energy-intensive industries: A review of current status, technologies and policies," *Energies*, vol. 14, no. 9, p. 2408, 2021.

[8] Countries, cities, carmakers commit to end fossil-fuel vehicles by 2040. [Online]. Available: https://www.reuters.com/business/cop/six-major-carmakers-agree-phase-out-fossil-fuel-vehicles-by-2040-uk-says-2021-11-10/

[9] D. L. Greene, E. Kontou, B. Borlaug, A. Brooker, and M. Muratori, "Public charging infrastructure for plug-in electric vehicles: what is it worth?" *Transportation Research Part D: Transport and Environment*, vol. 78, p. 102182, 2020.

[10] X.-G. Yang, G. Zhang, S. Ge, and C.-Y. Wang, "Fast charging of lithium-ion batteries at all temperatures," *Proceedings of the National Academy of Sciences*, vol. 115, no. 28, pp. 7266–7271, 2018.

[11] Key strategies to help cities overcome the charging challenge quickly, easily, and at lower cost. [Online]. Available: https://theicct.org/blog/staff/key-strategies-help-cities-overcome-charging-challenge-quickly-easily-and-lower-cost

[12] S. Hardman and G. Tal, "Understanding discontinuance among california's electric vehicle owners," *Nature Energy*, vol. 6, no. 5, pp. 538–545, 2021.

[13] S. Limmer, "Dynamic pricing for electric vehicle charging—a literature review," *Energies*, vol. 12, no. 18, p. 3574, 2019.

[14] "Sciurus: Domestic V2G demonstration," Centre of Excellence for Low Carbon and Fuel Cell technologies, Tech. Rep., 2021. [Online]. Available: https://www.cenex.co.uk/projects-case-studies/sciurus/

[15] S. Wu, R. Xiong, H. Li, V. Nian, and S. Ma, "The state of the art on preheating lithium-ion batteries in cold weather," *Journal of Energy Storage*, vol. 27, p. 101059, 2020.

[16] G. Zhang, S. Ge, X.-G. Yang, Y. Leng, D. Marple, and C.-Y. Wang, "Rapid restoration of electric vehicle battery performance while driving at cold temperatures," *Journal of Power Sources*, vol. 371, pp. 35–40, 2017.

[17] D. Hall, H. Cui, M. Bernard, S. Li, and N. Lutsey, "Electric vehicle capitals: Cities aim for all-electric mobility," 2020.

[18] S. Srdic and S. Lukic, "Toward extreme fast charging: Challenges and opportunities in directly connecting to medium-voltage line," *IEEE Electrification Magazine*, vol. 7, no. 1, pp. 22–31, 2019.

[19] T. Waldmann, M. Wilka, M. Kasper, M. Fleischhammer, and M. Wohlfahrt-Mehrens, "Temperature dependent ageing mechanisms in lithium-ion batteries–a post-mortem study," *Journal of Power Sources*, vol. 262, pp. 129–135, 2014.

[20] E. Figenbaum, "Battery electric vehicle fast charging–evidence from the norwegian market," *World Electric Vehicle Journal*, vol. 11, no. 2, p. 38, 2020.

[21] D. Ramsey, A. Bouscayrol, L. Boulon, and A. Vaudrey, "Simulation of an electric vehicle to study the impact of cabin heating on the driving range," in *2020 IEEE 91st Vehicular Technology Conference (VTC2020-Spring)*. IEEE, 2020, pp. 1–5.

[22] J. R. M. D. Reyes, R. V. Parsons, and R. Hoemsen, "Winter happens: The effect of ambient temperature on the travel range of electric vehicles," *IEEE Transactions on Vehicular Technology*, vol. 65, no. 6, pp. 4016–4022, 2016.

[23] "Understand how temperature affects how far your ev can go on a full battery." [Online]. Available: https://www.geotab.com/blog/ev-range/

[24] Y. Motoaki, W. Yi, and S. Salisbury, "Empirical analysis of electric vehicle fast charging under cold temperatures," *Energy Policy*, vol. 122, pp. 162–168, 2018.

[25] G. Liu, M. Ouyang, L. Lu, J. Li, and X. Han, "Analysis of the heat generation of lithium-ion battery during charging and discharging considering different influencing factors," *Journal of Thermal Analysis and Calorimetry*, vol. 116, no. 2, pp. 1001–1010, 2014.

[26] M. Keyser, A. Pesaran, Q. Li, S. Santhanagopalan, K. Smith, E. Wood, S. Ahmed, I. Bloom, E. Dufek, M. Shirk *et al.*, "Enabling fast charging–battery thermal considerations," *Journal of Power Sources*, vol. 367, pp. 228–236, 2017.

[27] K. Clement-Nyns, E. Haesen, and J. Driesen, "The impact of charging plug-in hybrid electric vehicles on a residential distribution grid," *IEEE Transactions on power systems*, vol. 25, no. 1, pp. 371–380, 2009.

[28] D. B. Richardson, "Electric vehicles and the electric grid: A review of modeling approaches, impacts, and renewable energy integration," *Renewable and Sustainable Energy Reviews*, vol. 19, pp. 247–254, 2013.

[29] I. Bayram, "Impacts of electric vehicle charging under cold weather on power networks," in *56TH INTERNATIONAL UNIVERSITIES POWER ENGINEERING CONFERENCE*, Aug 2021, pp. 1–6.

[30] I. S. Bayram and A. Tajer, *Plug-in Electric Vehicle Grid Integration*. Artech House, 2017.

[31] Z. J. Lee, S. Sharma, and S. H. Low, "Research tools for smart electric vehicle charging: An introduction to the adaptive charging network research portal," *IEEE Electrification Magazine*, vol. 9, no. 3, pp. 29–36, 2021.

[32] A. Moradipari and M. Alizadeh, "Pricing and routing mechanisms for differentiated services in an electric vehicle public charging station network," *IEEE Transactions on Smart Grid*, vol. 11, no. 2, pp. 1489–1499, 2019.

[33] Q. Tang, K. Wang, K. Yang, and Y.-s. Luo, "Congestion-balanced and welfare-maximized charging strategies for electric vehicles," *IEEE Transactions on Parallel and Distributed Systems*, vol. 31, no. 12, pp. 2882–2895, 2020.

[34] Y. Kim, J. Kwak, and S. Chong, "Dynamic pricing, scheduling, and energy management for profit maximization in phev charging stations," *IEEE Transactions on Vehicular Technology*, vol. 66, no. 2, pp. 1011–1026, 2016.

[35] I. S. Bayram, G. Michailidis, and M. Devetsikiotis, "Unsplittable load balancing in a network of charging stations under qos guarantees," *IEEE Transactions on Smart Grid*, vol. 6, no. 3, pp. 1292–1302, 2015.

[36] S. Wang, S. Bi, Y.-J. A. Zhang, and J. Huang, "Electrical vehicle charging station profit maximization: Admission, pricing, and online scheduling," *IEEE Transactions on Sustainable Energy*, vol. 9, no. 4, pp. 1722–1731, 2018.

[37] I. Zenginis, J. Vardakas, N. Zorba, and C. Verikoukis, "Performance evaluation of a multi-standard fast charging station for electric vehicles," *IEEE transactions on smart grid*, vol. 9, no. 5, pp. 4480–4489, 2017.

[38] S. Esmailirad, A. Ghiasian, and A. Rabiee, "An extended m/m/k/k queueing model to analyze the profit of a multiservice electric vehicle charging station," *IEEE Transactions on Vehicular Technology*, vol. 70, no. 4, pp. 3007–3016, 2021.

[39] I. S. Bayram, A. Tajer, M. Abdallah, and K. Qaraqe, "Capacity planning frameworks for electric vehicle charging stations with multiclass customers," *IEEE Transactions on Smart Grid*, vol. 6, no. 4, pp. 1934–1943, 2015.

[40] I. Zenginis, J. Vardakas, N. Zorba, and C. Verikoukis, "Performance evaluation of a multi-standard fast charging station for electric vehicles," *IEEE Transactions on Smart Grid*, vol. 9, no. 5, pp. 4480–4489, 2018.

[41] F. Varshosaz, M. Moazzami, B. Fani, and P. Siano, "Day-ahead capacity estimation and power management of a charging station based on queuing theory," *IEEE Transactions on Industrial Informatics*, vol. 15, no. 10, pp. 5561–5574, 2019.

[42] C. A. Courcoubetis and M. I. Reiman, "Pricing in a large single link loss system," in *Proc. of 16th International Teletraffic Congress*, Edinburgh, UK, June 1999.

[43] T. Başar and R. Srikant, "A stackelberg network game with a large number of followers," *Journal of optimization theory and applications*, vol. 115, no. 3, pp. 479–490, 2002.

[44] M. Yu and S. H. Hong, "A real-time demand-response algorithm for smart grids: A stackelberg game approach," *IEEE Transactions on smart grid*, vol. 7, no. 2, pp. 879–888, 2015.

[45] W. A. Massey and J. Pender, "Dynamic rate erlang-a queues," *Queueing Systems*, vol. 89, no. 1, pp. 127–164, 2018.

[46] V. B. Iversen and S. Stepanov, "Derivatives of blocking probabilities for multi-service loss systems and their applications," in *Next Generation Teletraffic and Wired/Wireless Advanced Networking*. St. Petersburg, Russia: Springer, Sept. 2007, pp. 260–268.

[47] W. J. Stewart, *Numerical solution of Markov chains*. CRC press, 2021.

[48] L. Kleinrock, *Queueing systems, volume 1:Theory*. wiley New York, 1975, vol. 66.

[49] J. Kaufman, "Blocking in a shared resource environment," *IEEE Transactions on Communications*, vol. 29, no. 10, pp. 1474–1481, 1981.

[50] R. R. Mazumdar, "Performance modeling, loss networks, and statistical multiplexing," *Synthesis Lectures on Communication Networks*, vol. 2, no. 1, pp. 1–151, 2009.